Journal of Organometallic Chemistry 694 (2009) 3943–3950

Contents lists available at ScienceDirect

Journal of Organometallic Chemistry

journal homepage: www.elsevier.com/locate/jorganchem

Mechanism of ketone hydrosilylation by Cu(I) catalysts: A theoretical study

Thomas Gathy, Daniel Peeters, Tom Leyssens *

Laboratoire de Chimie Quantique, Université Catholique de Louvain, Place Louis Pasteur 1, B-1348 Louvain-la-Neuve, Belgium

ARTICLE INFO

Article history:
Received 1 July 2009
Received in revised form 3 August 2009
Accepted 7 August 2009
Available online 18 August 2009

Keywords:
CuH(phosphine)$_{2/3}$ complexes
Cu(I) catalysis
Hydrosilylation
Catalytic cycle
Theoretical study

ABSTRACT

The plausibility of the catalytic cycle suggested for the hydrosilylation of ketones by Cu(I) hydrides has been investigated by a theoretical DFT study. A model system made up of a CuH$(PH_3)_2$ catalyst, acetone and SiH_4 gives us the necessary insight into the intrinsic reactivity of the system. This reactivity is confirmed, by introducing the more rigid CuH$[C_4H_4(PH_2)_2]$ catalyst, as well as tetra-coordinated, CuH$(PH_3)_3$ and CuH$(PH_3)[C_4H_4(PH_2)_2]$ compounds. Computations show the activation of the copper fluoride pre-catalyst, as well as both steps of the catalytic cycle to involve a 4 center metathesis transition state as suggested in literature. These results show the reaction to be favored by the formation of a Van der Waals complex resembling the transition states. The formation of these latter is induced by stabilizing electrostatic interactions between those atoms involved in the bond breaking and bond forming. Both steps of the actual catalytic cycle show a free energy barrier of about 10 kcal/mol with respect to the isolated reactants, hereby confirming the plausibility of the suggested cycle. We have found a substantial overall exothermicity of the catalytic cycle of about 35 kcal/mol.

1. Introduction

Selective reduction of unsaturated double bonds through homogenous catalysis, is of great interest in synthetic organic chemistry. It was not until the '70s, that the first Rh(I) based catalyst, used for reductive hydrosilylation of ketones and imines, yielding, respectively, alcohols and amines were developed [1–3]. The softer reaction conditions of hydrosilylation, turned out to be a major advantage over other reduction reactions, such as hydrogenation. The cost of Rh catalysts, however, formed a major stumbling-block for their large scale industrialization. Over the last two decades alternative efficient asymmetric hydrosilylation reactions using titanium [4–7], zinc [8,9], tin [10], titanocene [5,11], manganese [12], and copper [11,13–17] were developed.

In 1988, Stryker was the first to introduce the use of copper hydride complexes for the reduction of α,β-unsaturated compounds [18–20] using $[CuHPPh_3]_6$, as a stoichiometric reducing reagent. This so called "Stryker's reagent" calls for CuCl plus an equivalent of NaO*t*-Bu to generate CuO*t*-Bu. To avoid this extremely air-sensitive system advances have been made to form the Cu–H species *in situ* [21,16,17,22]. By using silanes, as a stoichiometric hydride, only catalytic quantities of the copper species are required (for a review of CuH-catalyzed reactions see Refs. [14,15,18,31] and references herein). Recently Lipshutz and Frieman [26] described a chiral CuH species, which is exceptionally stable and can be stored in solution if kept under argon. This so called "CuH in a bottle" can be used directly without *in situ* preparation of a CuH species. As this system is air-sensitive, *in situ* preparations of CuH systems remains attractive. As the goal of the current paper is to present a first computational mechanistic study of these systems, a system was chosen for which the CuH species is created *in situ*, as hereby one not only investigates the actual catalytic cycle, but also the activation mechanism of the pre-catalyst. CuF_2 systems were reported by Carreira and co-worker [27], as well as Riant and coworkers [28] as interesting precursors to copper hydride. These latter showed that a CuF_2/Binap recipe used for the hydrosilylation of ketones, leads to a CuH system, that is not only stable towards oxygen, but shows accelerated reduction upon injection of oxygen into the system [29]. These features make this type of system an interesting candidate for a mechanistic study.

A scheme has been proposed to explain the observed reactivity. This scheme involves the formation of a pre-catalyst through a two step process, starting of with the transformation of CuF_2 to a $FCu(PPh_3)_3$ complex, which through ligand exchange will lead to the final diphosphine ligand as presented in Scheme 1.

A σ-bond metathesis between the copper fluoride and the hydrosilylation reagent then expectedly generates the copper hydride species (Scheme 2) [30].

This catalyst then enters the suggested catalytic cycle [23–25] shown in Scheme 3. In this cycle, the copper hydride reacts with the ketone to form a copper alkoxyde. Next, the copper alkoxyde undergoes a σ-bond metathesis with the hydrosilylation agent to regenerate the Cu–H complex and the silyl ether.

To verify the plausibility of the above mentioned cycle, we use computational chemistry in this paper to examine energetic, electronic, and structural properties of the suggested cycle. Our calculations use two different models. First we consider, the CuH$(PH_3)_2$

* Corresponding author.
E-mail address: tom.leyssens@uclouvain.be (T. Leyssens).

0022-328X/$ - see front matter © 2009 Elsevier B.V. All rights reserved.
doi:10.1016/j.jorganchem.2009.08.017

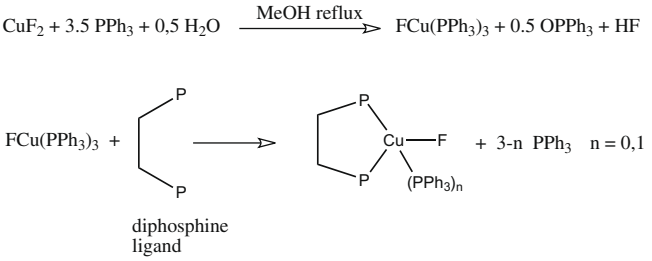

Scheme 1. Formation of the pre-catalyst.

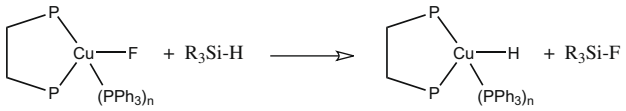

Scheme 2. Catalyst formation.

catalyst, which is convenient for a mechanistical study as it involves fewer atoms than the large catalytic systems used experimentally, but will give us the necessary insight into the intrinsic reactivity of the system. Using smaller systems facilitates the identification of stationary points. This would become cumbersome when using a true experimental system, without prior approximate knowledge of these points. Secondly, by introducing $CuH[C_4H_4(PH_2)_2]$ catalysts we strive towards a conformationally more rigid system. Doing so, one can determine whether or not the mechanism of the cycle studied is strongly affected by the nature of the diphosphine used. This information can guide further computational studies on large experimental systems. As concern might rise, whether or not the actual catalyst contains a supplementary PH_3 ligand, hence being tetra-coordinated, $CuH(PH_3)_3$ and $CuH(PH_3)[(C_4H_4(PH_2)_2]$ compounds are also considered.

2. Computational details

All structures were fully optimized using Becke's three parameter hybrid functional (B3LYP), as implemented in the GAUSSIAN 03 [32] series of programs. Optimized geometries are provided in the Supplementary material. Force constants were determined for the stationary points to characterize these latter, as well as to determine their entropies and free energies, based on a statistical thermodynamical treatment. Solvent effects are not yet included, as the main purpose of this paper is to verify the plausibility of the suggested mechanism. The Cu atom was described using an effective core potential to represent all but the valence *nd* and $(n+1)s$ and outer core *ns* and *np* electrons [33]. The latter were described with a triple zeta contraction of the original double zeta basis set, this combination is referred to as the LANL2DZ basis set. All non-metal atoms were described using the standard 6-31G(d,p) basis set (with only the five spherical harmonic d functions). Atomic charges were calculated using the NBO method [34]. As concern may rise concerning the adequacy of the chosen basis set, calculations using a larger, all electron basis set were performed for the $CuX(PH_3)_2$ model system.[1] Results (Table 2) show a consistent shift of about 5 kcal/mol for species involved in the transformation of the pre-catalyst to the catalyst, with respect to isolated reactants, and is due to a basis set superposition error involving the fluorine and silicon atoms.[2] This effect is no longer observed for the actual catalytic cycle (Tables 4 and 6). As the main objective of this paper is to study the plausibility of the actual catalytic cycle, with the possibility of transposing the basis set used to larger systems in order to study the enantioselectivity, the smaller basis set was chosen throughout this work.

3. Results and discussion

3.1. Formation of the pre-catalyst

The pre-catalyst is formed by placing a CuF_2/PPh_3 mixture at reflux in methanol. The structure of the formed $CuF(PPh_3)_3$ compound has been determined experimentally by X-ray diffraction of both the $FCu(PPh_3)_3{\cdot}2MeoH$ [36] and $FCu(PPh_3)_3{\cdot}2EtoH$ [37] solvates.[3]

Table 1 compares some theoretical and experimental bond lengths for these complexes.

Table 1 shows a shorter Cu–F bond compared to Cu–P bonds. The discrepancies between theoretical and experimental bond lengths, can be due to a multitude of effects, such as crystalline packing effects, or the fact that calculations have been performed in a gas phase model using the DFT level of theory.

Although Kagan and co-worker [38] showed that asymmetric hydrosilylation of ketones is possible using a Cu hydrate complex coordinated by monophosphine ligands, the low enantiomeric excess obtained, favored the use of diphosphine ligands. These latter were furthermore shown to have a positive influence on the reaction kinetics.

The diphosphine complexes are usually obtained by ligand exchange as presented in scheme 1. As mentioned above, in this paper we study the $CuH(PH_3)[(C_4H_4(PH_2)_2]$ complex to mimic these substances. The free energy difference (ΔG°) of −4.4 kcal/mol shows the overall process to be spontaneous.

3.2. Activation of the pre-catalyst

The active species for the selective reduction of ketones to alcohols is a copper hydride. This later is formed through a σ bond metathesis between the hydrosilane compound and the copper fluoride pre-catalyst. As shown on Fig. 1, the formation of a σ bond between the copper and hydrogen atom, occurs through transmetalation [18,17,30] passing by a 4 center transition state.

For the tetra-coordinated complexes, two energetically and structurally similar transition states are observed, which are connected through a Van der Waals complex being a mere 0.5 kcal/mol more stable than both transition states. This intermediate should therefore be considered as a very labile complex, that will not be observed experimentally and which origin can be related to the almost planar energy surface around the transition states. For simplicity the highest energy transition state will be discussed hereafter.

To arrive at the 4 center transition state, the pre-catalyst forms an energetically favored Van der Waals complex with the SiH_4 hydrogenating agent. Table 2 shows the relative energy, enthalpy

[1] For this system a TZVP [35] basis set was used for the Cu atom, and a 6-31++G(d,p) basis set for all other atoms. Structures were optimized using this basis set, and transition states checked for their validity.

[2] The BSSE for the $CuF(PH_3)_2/SiH_4$ and $CuH(PH_3)_2/CH_2O$ is a mere 1.5 kcal/mol using the TZVP/6-31++G(d,p) basis set, but increases to 3.8 kcal/mol for the $CuH(PH_3)_2/CH_2O$ and as high as 9.3 kcal/mol for the $CuF(PH_3)_2/SiH_4$ complex using the LANL2DZ/6-31G(d,p) basis set. This important BSSE for the CuF species can be reduced when introducing diffuse basis functions on the F atom. The BSSE contributes to an overestimation of the stabilization of these complexes with respect to isolated reactants. Excluding this contribution, the Van der Waal complexes remain stabilized with respect to isolated reactants, and the overall discussion therefore remains unaltered.

[3] Theoretical structures are given in Supplementary material.

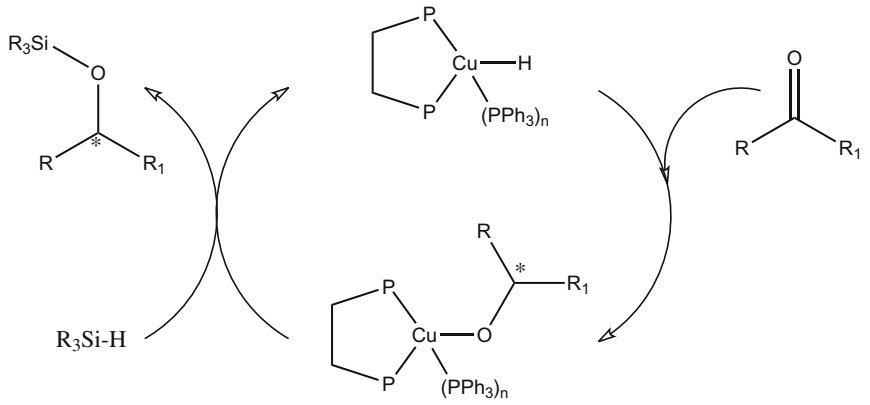

Scheme 3. Catalytic cycle.

Table 1
Experimental X-ray distances (Å) for $FCu(PPh_3)_3{\cdot}2MeOH$ and $FCu(PPh_3)_3.2EtOH$ and theoretical distances obtained for the $FCu(PH_3)_3$ complex.

Distance (Å)	$FCu(PPh_3)_3{\cdot}2MeOH$	$FCu(PPh_3)_3{\cdot}2EtOH$	$FCu(PH_3)_3$
Cu–F	2.11	2.06	1.87
Cu–P	2.32	2.32	2.39

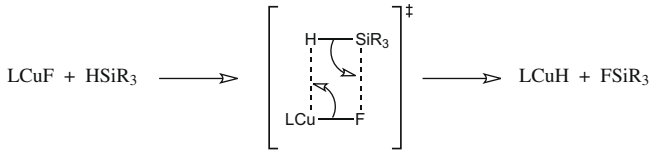

Fig. 1. Activation of the pre-catalyst.

and free energy of the Van der Waals complexes and transition states.

Table 2 shows, the formation of the initial Van der Waals complex between the copper fluoride pre-catalyst and the SiH_4 reactant to be energetically favored, although not spontaneous. The electrostatic interaction between the negatively charged fluorine atom and the positively charged copper atom, as well as the negatively charged hydrogen atom and the positively charged silicon atom as shown in Table 3, explains the driving force for this energetically favorable formation of the Van der Waals complex. The alignment of both dipoles orientates the formation of the 4 center transition state as shown on Fig. 2 for the $CuF[C_4H_4(PH_2)_2]$ – SiH_4 and $CuF(PH_3)_2$ – SiH_4 complexes.

As shown by Fig. 2 and Table 2 the transition states lie energetically and structurally close to the Van der Waals complexes. As expected for a σ bond metathesis, the transition states are characterized by increased Cu–F and Si–H bond lengths, while Cu–H and Si–F bonds become shorter.

Chemical reactions occur through reorganization of electron density between different nuclei. Investigation of how this density changes upon formation of the transition state therefore helps clarify the reaction mechanism. Fig. 3 shows the differential density between, respectively, the transition state, and the sum of both reactants at transition state geometry. Red and blue zones indicate, respectively, an increase and decrease in electron density. As shown on this figure, the transition state is characterized by a strong decrease of electron density around the copper atom, as well as a strong increase in the F–Si area, which corresponds to the breaking of the Cu fluoride bond, in favor of the formation of the Si–F bond. Although one observes a polarization of the electron density of the Si atom towards the hydrogen atom that will be transferred to the Cu atom, no significant increase in electron density is observed along the Cu–H axis at the transition state. The formation of the copper hydride bond and breaking of the Si–H bond is thus expected to be less advanced. The 4 σ bond metathesis can therefore be characterized as an asynchronous concerted reaction, with the breaking of the Cu–F bond in favor of the formation of the Si–F bond occurring slightly earlier than the transfer of the silicon linked hydrogen to the cupper atom.

For the formation to take place a free energy barrier of about 6 kcal/mol and 9 kcal/mol[4] has to be crossed for, respectively, the tri- and tetra-coordinated copper reactants.[5] The more important barrier for the tetra-coordinated copper pre-catalysts, can be explained by an increased steric effect and slight differences in bonding to the Cu atom explained by an additional σ donating and π acceptor effect of the phosphine ligand.

The activation mechanism of the pre-catalyst is exothermic by about 8 kcal/mol ($\Delta H^\circ = -8.10$ kcal/mol for the $CuF(PH_3)_2$) pre-catalyst) and spontaneous as shown by the difference in free energy of about −10 kcal/mol and −8 kcal/mol for, respectively, the tri- and tetra-coordinated copper reactants (Table 2). The fluorine atom seems essential to the activation of the pre-catalyst, as other copper halogen complexes show little to no reduction of ketones to alcohols. This observation could be explained by the less important electronegativity of the other halogen atoms, leading to less stabilized initial Van der Waals complexes due to decreased electrostatic interactions, but other factors such as bond strengths, steric effects, etc. could also be of importance. Further work is ongoing to understand these observations.

3.3. Catalytic cycle

Once activated, the copper hydride enters the catalytic cycle. The proposed mechanism for the hydrogenation of ketones by these hydride catalysts [14,15,31] occurs through a two step cycle as presented in Fig. 4. A first step concerns the formation of a copper alkoxyde, through a σ metathesis transition state similar to that observed for the activation of the pre-catalyst. In a second step, this alkoxyde reacts with a hydrosilane to yield a silylated ether, and the reactivated catalyst. Once more, the suggested mechanism passes through a four center transition state. The final alcohol is generated by hydrolysis of the silylated ether. Due to the fact that the alkoxyde complex is not observed experimentally the reduction of the ketone is suggested to be the rate limiting step [14].

[4] Free energy barriers are reported with respect to isolated reactants.

[5] Calculations were performed in the gas phase. As a consequence experimental ΔS° and ΔG° values are expected to be smaller.

Table 2
Relative energy (ΔE°), enthalpy (ΔH°) and free energy (ΔG°) with respect to pre-catalyst and SiH_4 reactants during the activation of the pre-catalyst. ΔE° (ΔH°, ΔG°) in kcal/mol. (Values in italic are those for the larger basis set (TZVP on Cu and 6-31++G(d,p) on all other atoms.)

Pre-catalyst	Van der Waals complex	TS	Van der Waals complex	Products
$CuF(PH_3)_2$	−6.5 (−4.2; 2.7)	−4.6 (−3.6; 4.9)	−10.8 (−9.2; −5.1)	−7.9 (−8.1; −10.7)
	−2.8 (−1.4; 8.5)	*0.1 (0.5; 11.4)*	*−5.2 (−4.7; 2.5)*	*−2.3 (−3.0; −2.6)*
$CuF[C_4H_4(PH_2)_2]$	−4.6 (−3.3; 3.64)	−3.6 (−3.3; 6.6)	−10.0 (−10.1; −2.0)	−7.3 (−7.9; −10.0)
$CuF(PH_3)_3$	−6.3 (−4.4; 4.8)	−4.1 (−3.2; 8.9)	−9.4 (−8.2; −0.4)	−7.7 (−8.4; −7.8)
$CuF(PH_3)[C_4H_4(PH_2)_2]$	−6.8 (−5.5; 4.2)	−3.4 (−3.3; 8.5)	−9.2 (−8.7; −1.0)	−6.5 (−7.1; −7.4)

Table 3
Atomic charges on F, Cu, Si, and H atoms for the initial Van der Waals complexes.

Pre-catalyst	F	Cu	Si	H
$CuF(PH_3)_2$	−0.71	0.72	0.85	−0.34
$CuF[C_4H_4(PH_2)_2]$	−0.72	0.72	0.67	−0.19
$CuF(PH_3)_3$	−0.72	0.72	0.75	−0.23
$CuF(PH_3)[C_4H_4(PH_2)_2]$	−0.72	0.74	0.77	−0.23

As for the activation of the pre-catalyst, a stabilizing Van der Waals complex is observed between the catalyst and the reacting ketone during the first step of the cycle. In this complex, the orientation of the molecules favors the formation of the 4 center transition state. Table 4 shows the relative energies, enthalpies, as well as free energies of the species involved in the first step of the catalytic cycle.

The results show the formation of the van de Waals complex to be energetically favored by about 5 kcal/mol. The slightly less important stabilization of the tetra-coordinated complexes could once more be due to an increased steric hindrance, as well as to changes in electronic density around the copper atom coming from interaction with the added phosphine ligand.

As shown on Fig. 6, the Van der Waals complexes are structurally close to the transition state activated complexes, hence explaining the small energetic differences between both. At the transition state the complexes are characterized by elongated, C–O and Cu–H bonds, as well as reduced Cu–O and C–H bonds.

As for the activation of the pre-catalyst, the density differences at the transition state (Fig. 5), point towards an asynchronous concerted reaction mechanism, with the Cu–H–C rearrangement being more advanced than the formation of the Cu–O bond. Fig. 5 shows a decrease in electron density along the Cu–H axis, as well as an increase along the H–C axis. The electron density of the C=O double bond is furthermore displaced towards a lone pair on the oxygen atom. In a second instance, this electronic density on the oxygen will be transferred to the Cu atom to complete the σ bond metathesis.

For the reaction to take place, a free energy barrier of about 10 kcal/mol with respect to the isolated reactants has to be crossed

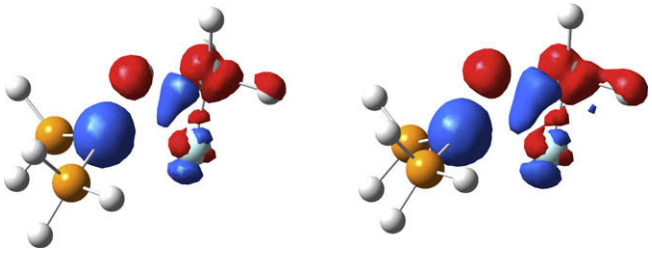

Fig. 3. Density difference between transition state and sum of reactants at transition state geometry. Red and blue zones indicate, respectively, an increase and decrease in electron density. Isodensity surfaces given at 0.01 and 0.008 e^-/V. Plots were made using the GAUSSVIEW program [39]. (For interpretation of the references to colour in this figure legend, the reader is referred to the web version of this article.)

which is more important than the barrier observed for the activation of the pre-catalyst. It can therefore be assumed that the total of the Cu–F species will have been transformed into Cu–H catalytical species at the onset of the ketone reduction. As for the activation of the pre-catalyst, the tetra-coordinated species are characterized by a slightly more important free energy barrier. A replacement of two PH_3 ligands by a diphosphine ligand, slightly lowers the free energy barrier. As shown on Fig. 6, an increase in P–Cu–P bond angle, could release the tension of the cisoid diphosphine ligand, hereby stabilizing the transition state with respect to reactants, and thus lower the free energy barrier. Such an effect of changes in bite angle on rate and selectivity is common to diphosphine ligands [40].

The formation of the copper alkoxyde is furthermore strongly exothermic (ΔH° = −26.3 kcal/mol for the $CuH(PH_3)_2$ molecule) (see Table 5).

The second step of the catalytic cycle concerns the regeneration of the catalyst, through the reaction of the Cu-alkoxyde species with a silane molecule, yielding a silylated ether product. As for the previous steps, a σ metathesis reaction is suggested with a 4 center transition state. Computations indeed show a stabilizing energetic interaction of about 5 kcal/mol (Table 6) between the al-

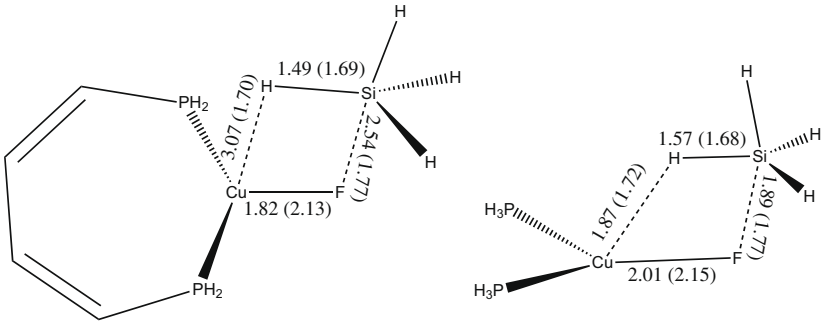

Fig. 2. Alignment of both dipoles for the $CuF[C_4H_4(PH_2)_2]$ – SiH_4 and $CuF(PH_3)_2$ – SiH_4. Bond lengths are given in Å for the Van der Waals complexes, as well as the transition states (between brackets).

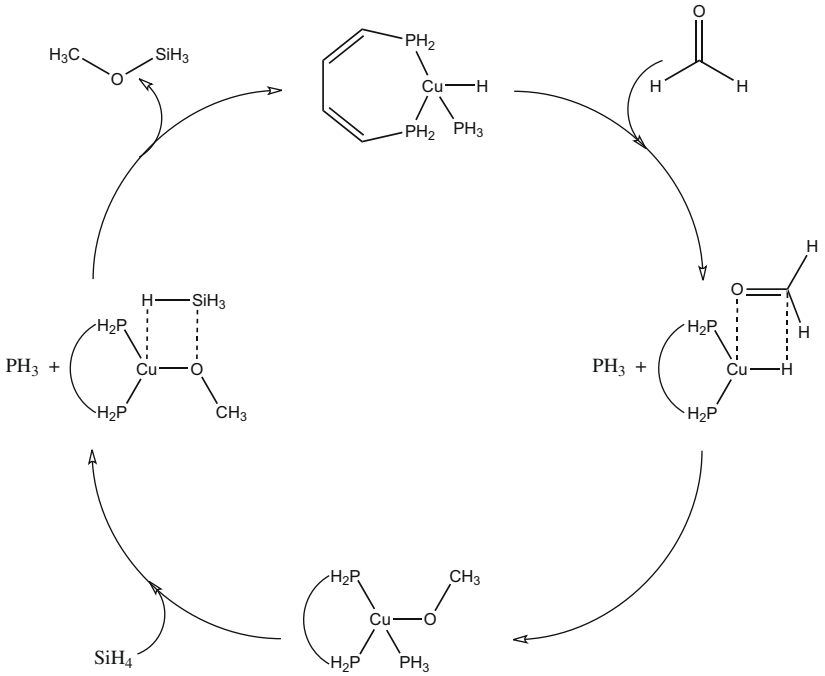

Fig. 4. The proposed mechanism for the hydrogenation of ketones by copper hydride catalysts.

Table 4
Relative energy ($\Delta E°$), enthalpy ($\Delta H°$) and free energy ($\Delta G°$) with respect to catalyst and ketone reactants during the first step of the catalytic cycle. $\Delta E°$ ($\Delta H°$, $\Delta G°$) in kcal/mol. (Values in italic are those for the larger basis set (TZVP on Cu and 6-31++G(d,p) on all other atoms.)

Catalyst	Van der Waals complex	TS	Products
$CuH(PH_3)_2$	−6.0	−3.1	−33.1
	(−4.9; 4.6)	(−1.8; 9.9)	(−27.9; −18.4)
	−6.2	*−4.5*	*−32.1*
	(−4.7; 6.0)	*(−3.4; 8.2)*	*(−27.2; −17.4)*
$CuH[C_4H_4(PH_2)_2]$	−5.3	−1.8	−32.8
	(−4.4; 5.1)	(−0.3; 8.5)	(−27.7; −15.9)
$CuH(PH_3)_3$	−4.8	−1.9	−31.2
	(−3.8; 5.1)	(−0.8; 11.9)	(−26.3; −16.2)
$CuH(PH_3)[C_4H_4(PH_2)_2]$	−4.8	−2.8	−32.1
	(−4.2; 5.7)	(−1.7; 10.2)	(−27.1; −16.8)

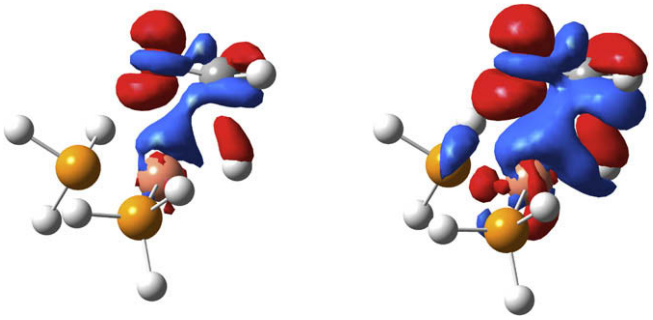

Fig. 5. Density difference between transition state and sum of reactants at transition state geometry. Red and blue zones indicate, respectively, an increase and decrease in electron density. Isodensity surfaces given at 0.004 and 0.002 e^-/V. Plots were made using the GAUSSVIEW program [39]. (For interpretation of the references to colour in this figure legend, the reader is referred to the web version of this article.)

koxyde catalyst and the silane molecule, which is comparable to the energetic stabilization observed for Van de Waals complexes obtained during the activation of the pre-catalytic CuF species, as well as that obtained during the first step of the catalytic cycle. This interaction orientates the compounds once more to the 4 center transition state, characterized by shortened Cu–H and Si–O bonds, as well as elongated Si–H and Cu–O bonds, as shown on Fig. 7.

Density differences (Fig. 8), once more indicate an asynchronous transition state with the Cu–O bond breaking/O–Si bonding being more advanced compared to the hydrogen transfer towards the Cu atom. Although a polarization of electron density from the silicon atom towards the transferable hydrogen is observed, no density increase is yet observed along the H–Cu axis.

For the reaction to take place, a free energy barrier of about 9 kcal/mol and 12 kcal/mol with respect to isolated reactants for, respectively, the tri- and tetra-coordinated complexes has to be crossed, comparable to the barriers observed during the activation of the pre-catalyst, as well as the first step of the catalytic cycle.

The comparable energy barriers for the two steps of the catalytic cycle are shown in Fig. 9 for the $CuH(PH_3)_2$ complex. They do not allow identifying the rate limiting step. Steric effects most likely have an increasing importance, for more complex diphosphine ligands (e.g. the binap ligand), as well as with increasing ketone size. The identification of the rate limiting step, will be discussed in future contributions. Energetic barriers, are nevertheless substantially lower than the free energy barrier of 50.16 kcal/mol calculated for the non catalyzed hydrosilylation of acetone. The low energetic barriers calculated in this work show the plausibility of the suggested catalytic cycle, and furthermore explain the high turnover number observed for these types of catalyst.

The tetra-coordinated species are once more characterized by a slightly more important free energy barrier. The second step of the catalytic cycle shows an exothermicity of ($\Delta H°$) −8.4 kcal/mol for the $CuH(PH_3)_2$ molecule, comparable to the exothermicity observed during the preparation of the catalysis from the CuF species. The overall catalytic cycle shows an exothermicity of about 35 kcal/mol ($\Delta H° = -34.7$ kcal/mol for the $CuH(PH_3)_2$ molecule), which is driven by the transformation of a π C=O bond and a σ Si–H bond, into more stable σ C–H and σ O–Si bonds.

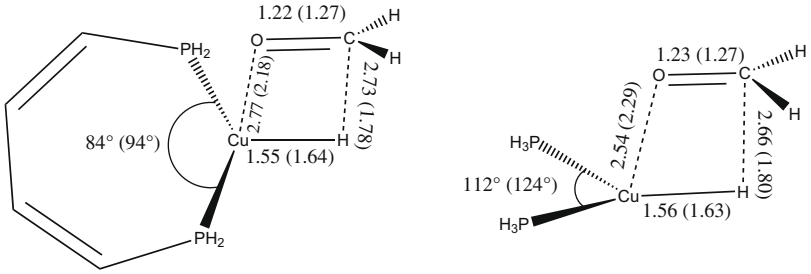

Fig. 6. Alignment of both dipoles for the $CuH[C_4H_4(PH_2)_2]$ – H_2CO and $CuH(PH_3)_2$ – H_2CO complexes. Bond lengths are given in Å for the Van der Waals complexes, as well as the transition states (between brackets).

Table 5
Atomic charges on H, Cu, C, and O atoms for the Van der Waals complexes at the first step of the catalytic cycle.

Catalyst	H	Cu	C	O
$CuH(PH_3)_2$	−0.49	0.55	0.12	−0.59
$CuH[C_4H_4(PH_2)_2]$	−0.47	0.47	0.15	−0.57
$CuH(PH_3)_3$	−0.55	0.60	0.20	−0.57
$CuH(PH_3)[C_4H_4(PH_2)_2]$	−0.53	0.57	0.21	−0.57

Table 6
Relative energy ($\Delta E°$), enthalpy ($\Delta H°$) and free energy ($\Delta G°$) with respect to alkoxyde catalyst and silane reactants during the second step of the catalytic cycle. $\Delta E°$ ($\Delta H°$, $\Delta G°$) in kcal/mol. (Values in italic are those for the larger basis set (TZVP on Cu and 6-31++G(d,p) on all other atoms.)

Catalyst	Van der Waals complex	TS	Products
$CuH(PH_3)_2$	−4.6 (−4.5; 7.4)	−4.1 (−3.4; 8.7)	−7.0 (−7.4; −6.7)
	−3.8 (−2.5; 9.0)	*−3.2 (−2.4; 10.1)*	*−6.2 (−6.5; −6.1)*
$CuH[C_4H_4(PH_2)_2]$	−4.8 (−4.6; 6.2)	−4.1 (−3.4; 8.2)	−7.3 (−7.5; −9.2)
$CuH(PH_3)_3$	−5.8 (−5.0; 6.0)	−2.8 (−1.6; 12.0)	−8.9 (−9.0; −8.9)
$CuH(PH_3)[C_4H_4(PH_2)_2]$	−6.0 (−5.3; 5.8)	−4.3 (−3.3; 7.0)	−8.0 (−8.1; −8.3)

4. Conclusions

In this paper, we have shown the theoretical validity of the suggested catalytic cycle for the hydrosilylation of ketones using Cu(I) hydride catalysts. The activation of the catalyst from a copper-fluoride complex, as well as both steps of the catalytic cycle involve a σ metathesis 4 center transition state. The reactants are guided towards these transition states, through the formation of energetically favored Van der Waals complexes, which energetically and structurally resemble the transition states. The driving force behind the formation of the Van der Waals complexes is a stabilizing electrostatic interaction. The transition states are characterized by an increase in bond length of those bonds that are breaking, and a decrease in bond length of the newly formed bonds. Density differences furthermore show that the σ metathesis reactions studied here should be described as asynchronous concerted mechanisms, with the transfer from Cu linked atoms being more advanced than the transfer towards this metal center.

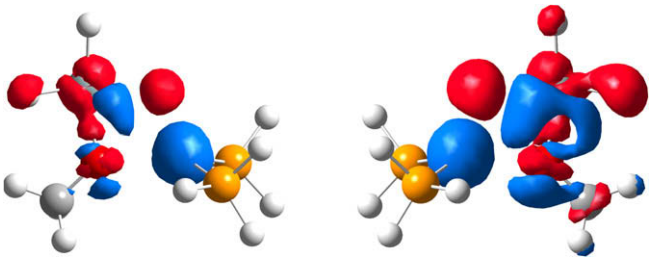

Fig. 8. Density difference between transition state and sum of reactants at transition state geometry. Red and blue zones indicate, respectively, an increase and decrease in electron density. Isodensity surfaces given at 0.008 and 0.004 e^-/V. Plots were made using the GAUSSVIEW program [39]. (For interpretation of the references to colour in this figure legend, the reader is referred to the web version of this article.)

For the reductive hydrosilylation of a acetone by SiH_4 to take place, a free energy barrier of about 10 kcal/mol with respect to the isolated reactants has to be crossed. Comparable energy barriers are obtained for the two successive steps of the actual catalytic cycle. To identify the rate limiting step, larger ligands will have to be introduced in order to account for the steric effects. Introduction of larger ligands, might also shown more important differ-

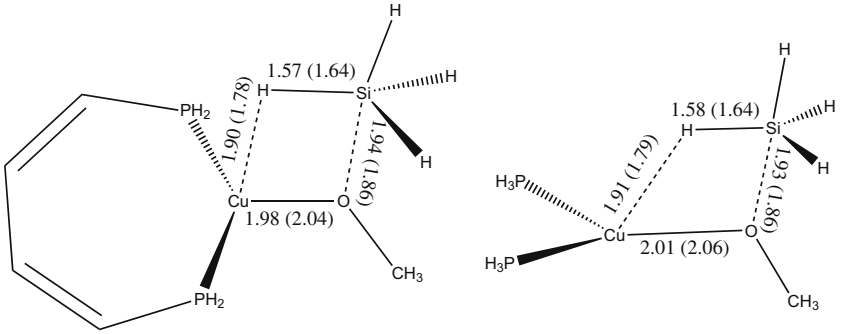

Fig. 7. Alignment of both dipoles for the $H_3COCu[C_4H_4(PH_2)_2]$ – SiH_4 and $H_3COCu(PH_3)_2$ – SiH_4. Bond lengths are given in Å for the Van der Waals complexes, as well as the transition states (between brackets).

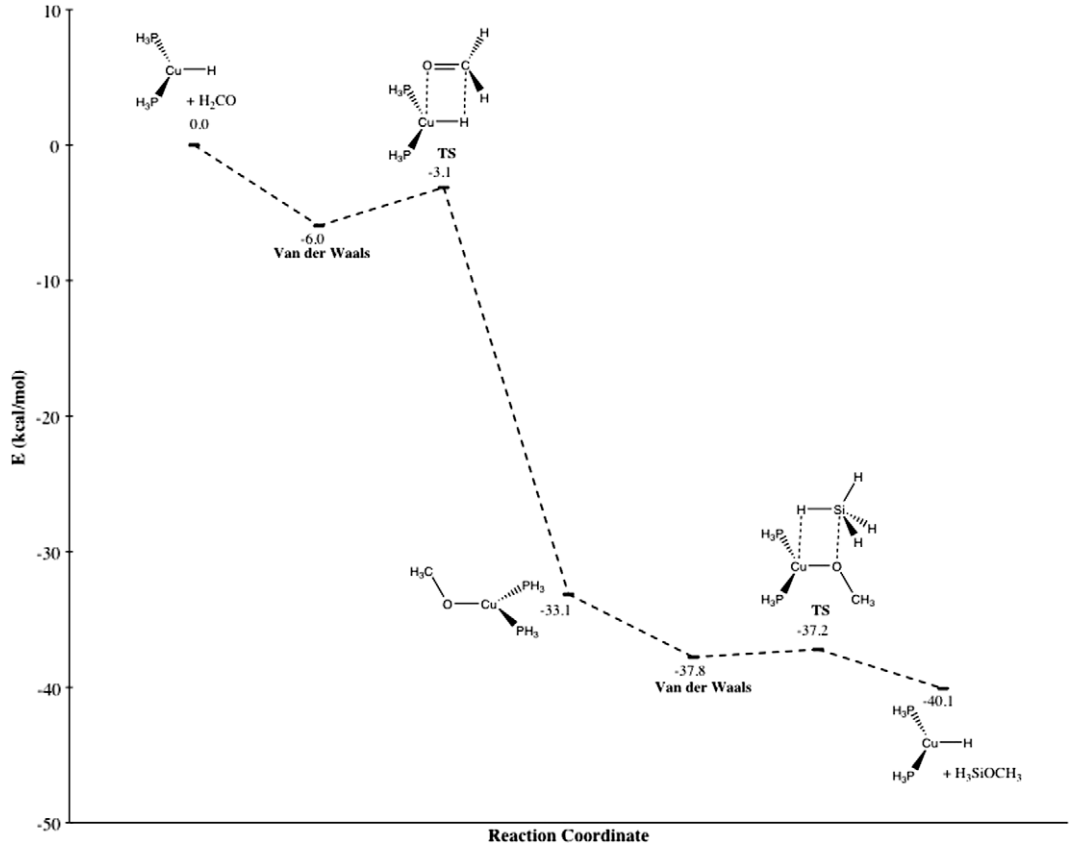

Fig. 9. Calculated B3LYP/6-31G** potential energy surface (kcal/mol) for the catalytic cycle of hydrosilylation of formaldehyde by the $HCu(PH_3)_2$ model catalyst.

ences between tri- and tetra-coordinated copper complexes, which show little to no difference for the small systems studied here. As mentioned previously, reduction by this system is accelerated by oxygen, invoking a possible change in nature of the catalyst. These points will be discussed in future work.

Finally, we have found a substantial overall exothermicity of the catalytic cycle of about 35 kcal/mol, driven by the transformation of a π C=O bond and a σ Si–H bond, into more stable σ C–H and σ O–Si bonds.

Acknowledgements

The authors are indebted to the Université Catholique de Louvain (Thomas Gathy), as well as the Belgian National Fund for Scientific Research (F.N.R.S.) for its financial support to this research (Tom Leyssens is a Postdoctoral Researcher). They would also like to thank the F.N.R.S for its support to access computational facilities project (Project No. 2.4502.05).

Appendix A. Supplementary material

Supplementary data associated with this article can be found, in the online version, at doi:10.1016/j.jorganchem.2009.08.017.

Reference

[1] I. Ojima, M. Nihonyanagi, Y. Nagai, J. Chem. Soc., Chem. Commun. (1972) 938.
[2] N. Langlois, T.P. Dang, H.B. Kagan, Tetrahedron Lett. 49 (1973) 4865.
[3] W. Dumont, J.-C. Poulin, H.B. Kagan, J. Am. Chem. Soc. 95 (1973) 8295.
[4] R. Halterman, T.M. Ramsey, Z. Chen, J. Org. Chem. 59 (1994) 2642.
[5] M.B. Carter, B. Schiott, A. Gutiérrez, S.L. Buchwald, J. Am. Chem. Soc. 116 (1994) 11667.
[6] J.F. Harrod, S. Xin, Can. J. Chem. 73 (1995) 999.
[7] H. Imma, M. Mori, T. Nakai, Synlett (1996) 1229.
[8] O. Riant, N. Mostefa, J. Courmarcel, Synthesis 18 (2004) 2943.
[9] H. Mimoun, J.Y. de Saint Laumer, L. Giannini, R. Scopelliti, C. Floriani, J. Am. Chem. Soc. 121 (1999) 6158.
[10] N. Lawrence, S.M. Bushell, Tetrahedron Lett. 41 (2000) 4507.
[11] J. Yun, S.L. Buchwald, J. Am. Chem. Soc. 121 (1999) 5640.
[12] S.U. Son, S.-J. Paik, I.S. Lee, Y.-A. Lee, Y.K. Chung, Organometallics 18 (1999) 4114.
[13] J. Wu, J.-X. Ji, A.S.C. Chan, Proc. Nat. Acad. Sci. 102 (2005) 3570.
[14] B.H. Lipshutz, W. Chrisman, K. Noson, J. Organomet. Chem. 624 (2001) 367.
[15] D.-W. Lee, J. Yun, Tetrahedron Lett. 45 (2004) 5415.
[16] B.H. Lipshutz, A. Lower, K. Noson, Org. Lett. 4 (2002) 4045.
[17] B.H. Lipshutz, C.C. Caires, P. Kuipers, W. Chrisman, Org. Lett. 5 (2003) 3085.
[18] W.S. Mahonney, D.M. Bretensky, J.M. Stryker, J. Organomet. Chem. 110 (1988) 291.
[19] J.-X. Chen, D.M. Daeuble, J.M. Stryker, Tetrahedron 56 (2000) 2789.
[20] J.-X. Chen, D.M. Daeuble, J.M. Stryker, Tetrahedron 56 (2000) 2153.
[21] B.H. Lipshutz, K. Noson, W. Chrisman, J. Am. Chem. Soc. 123 (2001) 12917.
[22] B.H. Lipshutz, K. Noson, W. Chrisman, A. Lower, J. Am. Chem. Soc. 125 (2001) 8779.
[23] B.H. Lipshutz, in: N. Krause (Ed.), Modern Organocopper Chemistry, Springer, Weinheim, 2002, pp. 167–187. and references cited therein.
[24] S. Rendler, M. Oestreich, Angew. Chem., Int. Ed. 46 (2007) 498.
[25] C. Deutsch, N. Krause, B.H. Lipshutz, Chem. Rev. 108 (2008) 2916.
[26] B.H. Lipshutz, B.A. Frieman, Angew. Chem. 117 (2005) 6503;
B.H. Lipshutz, B.A. Frieman, Angew. Chem., Int. Ed. 44 (2005) 6345.
[27] (a) C. Czekelius, E.M. Carreira, Org. Process Res. Dev. 11 (2007) 633;
(b) C. Czekelius, E.M. Carreira, Org. Lett. 6 (2004) 4575;
(c) C. Czekelius, E.M. Carreira, Angew. Chem. 115 (2003) 4941;
(d) C. Czekelius, E.M. Carreira, Angew. Chem., Int. Ed. 42 (2003) 4793.
[28] (a) S. Sirol, J. Courmarcel, N. Mostefa, O. Riant, Org. Lett. 3 (2001) 4111;
(b) J. Courmarcel, N. Mostefa, S. Sirol, S. Choppin, O. Riant, Israel J. Chem. 41 (2001) 231.
[29] N. Mostefa, S. Sirol, J. Courmarcel, O. Riant, Israel Synth. 349 (2007) 1797.
[30] H. Ito, T. Ishizuka, T. Okumura, H. Yamanaka, J. -I Tateiwa, M. Sonoda, A. Hosomi, J. Organomet. Chem. 574 (1999) 102.
[31] H. Kaur, F. Zinn, E.D. Stevens, P.S. Nolan, Organometallics 23 (2004) 1157.
[32] GAUSSIAN 03, Revision C.02, M.J. Frisch, G.W. Trucks, H.B. Schlegel, G.E. Scuseria, M.A. Robb, J.R. Cheeseman, J.A. Montgomery Jr., T. Vreven, K.N. Kudin, J.C. Burant, J.M. Millam, S.S. Iyengar, J. Tomasi, V. Barone, B. Mennucci, M. Cossi, G. Scalmani, N. Rega, G.A. Petersson, H. Nakatsuji, M. Hada, M. Ehara, K. Toyota, R. Fukuda, J. Hasegawa, M. Ishida, T. Nakajima, Y. Honda, O. Kitao, H. Nakai, M. Klene, X. Li, J.E. Knox, H.P. Hratchian, J.B. Cross, V. Bakken, C. Adamo, J.

Jaramillo, R. Gomperts, R.E. Stratmann, O. Yazyev, A.J. Austin, R. Cammi, C. Pomelli, J.W. Ochterski, P.Y. Ayala, K. Morokuma, G.A. Voth, P. Salvador, J.J. Dannenberg, V.G. Zakrzewski, S. Dapprich, A.D. Daniels, M.C. Strain, O. Farkas, D.K. Malick, A.D. Rabuck, K. Raghavachari, J.B. Foresman, J.V. Ortiz, Q. Cui, A.G. Baboul, S. Clifford, J. Cioslowski, B.B. Stefanov, G. Liu, A. Liashenko, P. Piskorz, I. Komaromi, R.L. Martin, D.J. Fox, T. Keith, M.A. Al-Laham, C.Y. Peng, A. Nanayakkara, M. Challacombe, P.M.W. Gill, B. Johnson, W. Chen, M.W. Wong, C. Gonzalez, J.A. Pople, GAUSSIAN, Inc., Wallingford CT, 2004.

[33] P.J. Hay, W.R. Wadt, J. Chem. Phys. 82 (1985) 720.

[34] (a) J.P. Foster, F. Weinhold, J. Am. Chem. Soc. 102 (1980) 7211;
(b) A.E. Reed, F. Weinhold, J. Chem. Phys. 78 (1983) 4066;
(c) A.E. Reed, R.B. Weinstock, F. Weinhold, J. Chem. Phys. 83 (1985) 735;
(d) A.E. Reed, F. Weinhold, J. Chem. Phys. 83 (1985) 1736.

[35] (a) A. Schaefer, H. Horn, R. Ahlrichs, J. Chem. Phys. 97 (1992) 2571;
(b) A. Schaefer, C. Huber, R. Ahlrichs, J. Chem. Phys. 100 (1994) 5829.

[36] P.C. Healy, J.V. Hanna, J.D. Kildea, B.W. Skelton, A.H. White, Aust. J. Chem. 44 (1991) 427.

[37] D.J. Gulliver, W. Levason, M. Webster, Inorg. Chim. Acta 52 (1981) 153.

[38] F. Lagasse, H.B. Kagan, Chem. Pharm. Bull. 48 (2000) 315.

[39] T. Keith, J. Millam, GAUSSVIEW, Version 4.1.2, R. Dennington, II, Semichem, Inc., Shawnee, 2006.

[40] P.W.N.M. Van Leeuwen, P.C.J. Kamer, J.N.H. Reek, P. Dierkes, Chem. Rev. 100 (2000) 2741.